Synthesis, Sintering and dielectric properties of ZnO-NiO-SiO_2 –xZrO2 (x=1-10)

Osama A. Desouky

Bilbis Higher Institute of Engineering (BHIE), Bilbis, Sharqia, Egypt

Abstract

Bulk (Zn Ni Si Zr) O_2 were synthesized by the standard ceramic method, with solid state reaction . The effect of ZrO2 on physical, phase structure and dielectric properties were investigated .Phase quantification and compositional studies were performed using X-Ray Diffraction patterns, Scanning Electron microscopy are discussed. The results show solid solution forms .Ni-rich phase. The SEM picture indicates the size of polycrystalline particles. The observation of some larger nano particles may be attributed to the fact that NiO nanoparticles have the tendency to agglomerate due to their high surface energy and high surface tension of the ultrafine nanoparticles. The decrease of capacitance in (pF) , dielectric constant (ε^- **)** and consequently increase (Ac) conductivity with increasing frequency was investigated .

Introduction

Zirconia-based materials are most interesting from a technological point of view, mainly as a consequence of their outstanding electrical, chemical, and mechanical properties that make them useful materials in the fields of ceramics, solid electrolytes, gas sensors, and catalysis [1-5]. Decreasing the size of the zirconia-based particles to nanometric levels provides changes in such properties due to the modifications produced at structural or electronic levels, as will be analyzed below. Thus, aspects such as the stabilization of the tetragonal structure (presenting higher ionic conductivity and strength with respect to the monoclinic polymorph), improved sintering characteristics, increased surface area, or modified mechanical properties (possibility of achieving superplastic characteristics, decreased fracture toughness, etc.) are characteristic of the zirconia based nanoparticles and most relevant for their practical use [5- 12]. Pure bulk zirconia exhibits three structures in different ranges of temperature at atmospheric pressure (other different orthogonal-type structures can be stabilized at high pressure) [13]. The most stable thermodynamic form is monoclinic and transforms to unquenchable tetragonal and cubic (fluorite) structures at 1400 and 2700 K (up to the melting point of ca. 2950 K), respectively [14, 15]. The stability of the monoclinic phase in the extended material has been explained on the basis

of covalency effects since a simple ionic model is inadequate to explain the observed structures [16]. A significant consequence of decreasing the size of pure zirconia is the possibility of stabilizing the tetragonal phase for particles of less than 30 nm [6, 7]. zirconia can be achieved upon introduction of cationic dopants[14,17,18,19].The amount of dopant required for the tetragonal stabilization in the nanoparticles generally depends on the nature of the dopant; a comparative study employing different rare-earth M^{3+} dopants shows that it decreases with increasing the ionic size of the dopant.[14,17] . The nature of the dopant also affects the oxide ion conductivity in the nanoparticles, which, as observed for the extended systems [18], increases with decreasing the ionic radius of the rare-earth dopant[19]. The use of zirconia nanoparticles as starting material in the preparation of dense oxygen permeation membranes presents advantages since they exhibit improved sintering behavior [14,18,20]. Transition metal-doped metal oxide nanocrystals have attracted considerable interest in the scientific community due to their unique optical and electro-optical properties. Among them, zinc oxide (ZnO) which has awide band gap (3.37 eV) and high exciton binding energy (60 meV) is a potential host material for doping transition metal ions [21]. Various theoretical and experimental studies on ZnO reveal a much wider scope in terms of nanocrystals shapes (wire, rod, cone and spherical), lattice structures, doping, surface modifications as well as synthesis conditions for tailoring the physical and optical properties of these nanocrystals [22-25]. Various dopants such as transition metals, Mn, Fe, Co and Ni, and rare earth elements, Eu, Er and Tb, have successfully been incorporated into the colloidal semiconducting nanocrystals (ZnO) for tailoring their characteristic properties [26]. Silicon dioxide (silica) is an oxide of silicon with the chemical formula SiO2. It is known for its hardness and three crystalline forms (quartz, tridymite and cristobalite). Often it would occur as a non-crystalline oxidation product. Silica is one of the most abundant oxide materials in the earth's crust and occurs commonly in nature as sandstone, silica sand quartzite. Silicate glasses and ceramics can exist in an amorphous form (vitreous silica) or in a variety of crystalline forms [27]. Silica generally has good abrasion resistance, electrical insulation and good thermal stability. It had been found that adsorption of water enhances the surface electrical conductivity of silica [28]. A fused silica is mainly used where good dielectric and insulating properties are required, though it may also be used as refractory materials or investment casting. Quartz is an insulator with band gaps in excess of 6 eV commonly used as substrates for supported catalysts. The electrical and optical properties of silica are strongly dependent on size, especially when formed into nanotubes, nanowires and nanoparticles due to their quantum confinement effect. Their different

applications are also shape dependent.[29-31] . NiO is the most exhaustively investigated transition metal oxide. It is NaCl-type antiferromagnetic oxide semiconductor. It offers promising candidature for many applications such as solar thermal absorber, catalyst for oxygen evolution, photo electrolysis and electro chromic device. Nickel oxide is also a well-studied material as the positive electrode in batteries. NiO is a P-type semiconductor and its electrical conduction is almost entirely contributed from electron hole conduction. NiO is preferred for high electro chromic efficiency, low cost and high dynamic dispersion. NiO on the other hand is a transition metal oxide that has several potential applications, such as solar thermal absorber, electrodes for battery and photoelectron-catalysts [32][15]. NiO thin films are promising materials with excellent electrochromic properties. Another important application of Nickel oxide films includes preparation of alkaline batteries (as cathode material), antiferromagnetic layers and P-type transparent conducting films [33][16]. The appealing electronic properties of NiO such as large band-gap energy of (≈ 4.00) EV, and high thermal stability, make it a favorable material for electronic device applications [34] .The study of composite material i.e. mixture consisting of at least two phases of different chemical composition has been of great interest from both fundamental and practical point of view. The physical properties of such materials can be combined to produce material of desired response. Composites have good potential for various industrial fields because of their excellent properties such as high hardness, high melting point, low density, low coefficient of thermal expansion, high thermal conductivity, good chemical stability and improved mechanical properties such as higher specific strength, better wear resistance and specific modulus. Composites are used in making solar cells, optoelectronic device elements, laser diodes and light emitting diodes (LED), industrial applications in aircraft, military and car industry. High-k gate dielectrics substituting for SiO2 gates in sub-100-nm metal-oxide-silicon field-effect transistors have been studied extensively recently because the conventional SiO2 dielectric faces scaling limits due to excessive gate tunneling current in the coming generations. One of the most promising candidates is ZrO2 [35- 39] due to its high dielectric constant, wide energy band gap [40], and thermodynamic stability in contact with Si [41]. However, pure amorphous ZrO2 crystallizes at around 500 ^{0}C, and so the deposited ZrO2 layer becomes crystalline after annealing in conventional integrated circuit processes. Composites are used in making solar cells, optoelectronic device elements, laser diodes and light emitting diodes (LED), industrial applications in aircraft, military and car industry. Besides this, the composites getting from the transition metal oxides are started to use as humidity and gas sensors.

Other work carried out in this area includes synthesis and characterization of ZnO-NiO composite nano particles by solution method[42] .While in this paper the influence of sintering temperature on the physical properties of ZnO – NiO- SiO2- ZrO2 composite prepared by solid state technique were characterized.

Materials and methods

Composite samples were fabricated by the conventional ceramic fabrication procedure. The starting materials selected were ZnO,SiO2 and ZrO2 in powder form and all materials were taken in the form of analytical grade . The mixes were weighed in the suggested proportions,

Batches were abbreviated as Z1, Z2, Z3, Z4, Z5, and Z6 (see Table 1) ,

wet milled to ensure through mixing of the different compositions then dried at 200 ^{o}C. Green cylindric compacts were uniaxially pressed at 70 KN into discs with a diameter of 20 mm and a thickness of 2 mm. The pellets were calcined at (1000 – 1300) °C for 2 h and cooled to room temperature freely, whereas the heating rate to the sintering temperature was typically 5°C/min. The sinterability of the different samples was determined in terms of physical properties. The phases developed during firing were identified by XRD utilizing an equipment; Philips type 1700, copper radiation and a Ni filter. Microstructure developed was examined under SEM type Philips XL 30 provided with EDS after sputtering the surface with gold. The dielectric properties and conductivity as a function of frequency were measured in centered Gold electrode pellet with a typical Impedance analyzer (Agilent 4292) in the frequency range 50 Hz–5 MHz .The capacitance and resistance were measured at room temperature and the respective permittivity [ε\] and conductivity [σ] were calculated according to the following relations :

$$\varepsilon^{-} = \frac{C\,d}{\varepsilon_o\,A}$$

Where C = capacitance In farad. d = thickness of specimen in m.

ε_o = dielectric constant of vacuum 8.85×10^{-12} F/m.

A = area of specimen in m^2.

Also from the values of resistance [R], the resistivity [ρ] and conductivity [σ] were calculated from the following relation:

$$\text{Resistivity } [\rho] = \frac{R\,A}{d} \qquad \text{Conductiviy } (\sigma) = \frac{1}{\rho}$$

To investigate the sintering mechanisms, an as-received powder sample was analyzed by the thermo gravimetric method. Concerning DTA, 40µm powder specimens were placed in a refractory steel crucible and analyzed using a hybrid system with oven-drying at a heating rate of 5.8 ^{o}C/min up to 600 ^{o}C. Sample masses ranged from 15 to 20 mg. In the case of TG, the specimen (40 µm powder) were introduced into a quartz crucible and analyzed using system at a heating rate of 7.5^{o}C/min up to 600^{o}C , under an atmospheric condition.

Results and Discussion

The relative density for the fired samples in the temperature range between 1000 and 1300 ◦C is illustrated in Fig. 1 . The relative density equals the theoretical density of a sample divided by its apparent density. The relative density for the samples decreased as the ZrO2 content increased. Although high densification rate in all samples took place at 1300 ◦C, it is interesting that only samples Z2, Z3, Z4 and Z6 have better sintering behavior. At 1300 ◦C, the relative density of samples Z2 and Z6 have reached 95%, which indicates that samples Z2, Z4 and Z6 get to almost full densification. Such a high rate of densification for samples Z2 and Z6 is thought to be attributed to the lowest glass transition temperature and the viscous glass phase during the firing process .

XRD patterns of samples sintered at 1200 ^{0}C are shown in Fig. 2. It is easy to identify the main phase willemite $Zn_2(SiO_4)$ (PDF card no 01-070-1235) as the major phase, M: Baddeleyite ZrO2 , Zircon(Zr2SiO4, PDF card no. 01-081-0588), B: Liebenbergite Ni_2SiO_4 and Nickel zinc oxide , zinc silicate and nickel silicate by fitting d spacing data. Additional peaks are evident and their intensity increases with increasing ZrO_2 . These additional peaks (Zr-rich phase) belong to two kinds of phases: one is Baddeleyite ZrO2 can be observed at about 2θ=28.391(d=3.14116)(07-0343) and Zircon, Zr(SiO4) , tetragonal structure, can be detected at about 2θ =20.026(d=4.43038), and 2θ =27.013(d=3.29813)(76-0865). The results show that Zn2SiO4 and Ni2SiO4 generate during sintering, but the d-spacing data do not exactly match with those of JCPDS card.

Fig. 3 . shows the differential thermal analysis DTA thermo gram of sample Z6 which containing 30%wt ZnO, 30%wt NiO, 30%wt SiO2 and1%wt ZrO2.The thermo gram shows

endothermic effect in which, the onset of the peak at 36.2ºC , the offset at 298.3 ºC, the mix ⁄ min at 109.5 ºC is equal to -16.817µv, and heat change is equal to -1503.706 µVs⁄mg. Fig. 4 .shows the TG thermo gram of sample Z6 , in which, mass of the sample at 56.3 ºC is equal to 9.056 mg, mass of the sample at 207.5 ºC is equal to 8.493 mg, and mass change is equal to -0.56 mg. In addition, mass of the sample at 207.5 ºC is equal to 8.493 mg, mass of the sample at 268.9 ºC is equal to 7.975 mg, and mass change is equal to -0.52 mg. In addition, mass of the sample at 268.9 ºC is equal to 7.975 mg, mass of the sample at 344.2 ºC is equal to 7.758 mg, and mass change is equal to -0.22 mg.

Figs.(5-13) Typical SEM photographs of the products synthesized through the stoichiometric and the Ni and Si -rich precursors: clusters of tiny particles and thin flakes imaged at a higher magnification. Elementary composition analysis by EDS confirms that the Ni content is higher near the grain boundary than in the matrix (ZnO), indicating the formation of a Ni and Zr-rich phase along the ZnO grain boundaries. Also SEM images of the as-prepared ZnO-NiO-SiO2 based composite ceramics also confirmed the solubility of ZrO2 into ZnO lattice. The images reveal that, although amount with different amounts of ZrO2, the typical microstructure of the samples almost has no change: almost fully dense structure of ZnO grains without any obvious second phases. Both images show evidence of the presence of a liquid phase as well as relatively small grains, with an average size clearly below the micron (similar to the particles sizes of the starting materials. Fig. 8 shows the SEM micrograph of two systems considered in this study. Although no secondary phases were observed in SEM micrographs, Ni_2SiO_4 and Zr_2SiO_4 could be precipitated at the grain boundaries leading to a decrease in the grain size with the increase in ZnO concentration. SEM of sample Z4 which containing (36ZnO-30NiO-30SiO2-4ZrO2) fired at 1000^{o}C, 1100^{o}C, 1200^{o}C, and 1300^{o}C, for 2 hours present in Fig. 9. The SEM picture indicates the size of polycrystalline particles. The observation of some larger nano particles may be attributed to the fact that NiO nanoparticles have the tendency to agglomerate due to their high surface energy and high surface tension of the ultrafine nanoparticles. The fine particle size results in a large surface area that in turn, enhances the nanoparticles catalytic activity. So we can conclude that the prepared NiO particles are in nanometer range. The agglomeration of nanocrystalline particles could be attributed to their extremely small dimensions with high surface energy during firing. Fig . 12 .SEM of sample Z5 sintered at 1200 ^{0}C revealed the presence of uniform grains larger than 7µm, while energy dispersive spectroscopy (EDAX) indicated the presence of Zn, Ni and Zr distributed inside the grains.

The dielectric properties of $ZnO\text{-}SiO_2\text{-}NiO\text{-}ZrO_2$ composite ceramic system were studied in the frequency range from 50 Hz to 5 MHz at room temperature. Figs. (14-16) show the variation of the dielectric constant as a function of frequency for all samples. Obviously, the dielectric constant shows a decreasing trend for all the samples. The decrease is rapid at lower frequency and slower and stable at higher frequency. The decrease of dielectric constant with increasing frequency is a normal dielectric behavior which is also observed by other researchers [43-46]. A composite ceramic system is considered as heterogeneous material that can experience interfacial polarization as predicted by Maxwell and Wagner. The movement of charge carriers trapped at interfacial region which is caused by inhomogeneous dielectric structure. At high frequency, the dominant mechanism contributing to dielectric constant is the hopping mechanism in their respective interstice under the influence of alternating current. The frequency of hopping between ions could not follow the frequency of applied field and hence it lags behind, therefore the values of dielectric constant become reduced at higher frequency [47]. This behavior may be due to existence of interfacial polarization , which exists in non-homogeneous dielectric . For samples sintered at 1200 for 2 hours , which containing SiO2, NiO, ZnO and ZrO2 ,the measured data show that the dielectric constant decrease generally with increasing frequencies. The sample (Z5) which containing 35% mole ZnO, 30% mole SiO2, 30% mole NiO and 5% mole ZrO2 represent the maximum values of dielectric constant. The results of dielectric loss as a function of frequency at room temperature of different mixes sintered at 1200 ^oC for 2hours are graphically plotted in Fig. . It is evident that mixes of different mixes show clearly decrease behavior with increasing frequency. The dielectric loss decreases in the frequency range up to 10 KHz; after 10 KHz becomes constant .This decreasing can be explained by Koop's model. According to Koop's model the decrease of dielectric loss (ε'') is explained by the fact that at lower frequencies, where the resistivity is high and the grain boundary effect is dominant, thus more energy is required to for the exchange of electrons between the metal ions and dopants ions located at grains boundaries ,i.e. energy loss is high whereas, at high frequencies, the resistivity is comparatively lower and grains themselves play a dominant role, thus very small amount of energy is required for hopping of electrons between the ions located in a grain, and therefore dielectric loss (ε'') is also small.

The effect of frequency on the resistivity of different mixes which containing ZnO, SiO2, NiO and 1, 2, 3, 5, 10 %mole ZrO2 sintered at 1200 ^0C for 2hours are graphically plotted in Fig. 16 . , generally the resistivity deceases with increasing of frequency of all specimens. This may be attributed

to the increase in the number of dipoles. These effects are associated with polarization currents arising from trapping states of various kinds and densities. The increase in frequency raised the conductivity as a result of the increase in ionic response to the field again this is related to inter-granular material.

Conclusions

1) The relative density for the samples decreased as the ZrO2 content increased.
2) The SEM picture indicates the size of polycrystalline particles. The observation of some larger nano particles may be attributed to the fact that NiO nanoparticles have the tendency to agglomerate due to their high surface energy and high surface tension of the ultrafine nanoparticles.
3) (EDAX) indicated the presence of Zn, Ni and Zr distributed inside the grains.
4) A composite ceramic system is considered as heterogeneous material that can experience interfacial polarization as predicted by Maxwell and Wagner.

5) The dielectric constant shows a decreasing trend for all the samples, the decrease is rapid at lower frequency and slower and stable at higher frequency.

6) The AC resistivity decreases with increasing frequency at room temperature. This may be attributed to the increase in the number of dipoles and consequently increases the hopping probability.

References

[1] A. H. Heuer, L. Hobbs, W.Eds.; The American Ceramics Society,Westerville, OH (**1981**) 3.

[2] Steele B C H, Heinzel A.Materials for fuel –cell technololgies. Nature 414 ,345-352 (**2001**).

[3] Brailsford, A. D., & Logothetis, E. M."Selected aspects of gas sensing". Sensors Actuators B 52 (1), 195-203 (1998).

[4] Somov SI, Reinhardt G, Guth U, Gopel W ." Multi-electrode zirconia electrolyte amperometric sensors" . Solid State Ionics, 136-137, 543- 547 (2000)

[5] Wolfram Stichert and Ferdi Schüth . "Influence of Crystallite Size on the Properties of Zirconia"*Chem. Mater.*, 10 (7) 2020–2026 (1998)

[6] Ronald C. *Garvie*. "Crystallite Size Effect". J. Phys. Chem. , 69 (4) 1238–1243(1965).

[7] A. Clearfield. "Crystalline Hydrous Zirconia". Inorg. Chem., 3 (1) 146–148 (1964).

[8] Mitsuhashi, T., Ichihara, M., *and* Taksuke, U., "Characterization and Stabilization of Metastable Tetragonal ZrO2, " J. Am. Ceram. Soc 57, 97–101 (1974).

[9] Garvie. R. C." Stabilization of the tetragonal structure in zirconia microcrystals". J. Phys. Chem., 82 (2) 218–224 (1978)

[10] Baldinozzi. G, Simeone. D, Gosset. D and Dutheil M. Neutron ."Diffraction Study of the Size-Induced Tetragonal to Monoclinic Phase Transition in Zirconia Nanocrystals'' Phys. Rev. Lett. 90, 216, 103 (2003).

[11] Mayo. M.J, Seidensticker J.R, Hague. D.C, Carim A.H., " Surface oxide ceramics". Nanostruct. *Mater.*, 11, (2) 271-282*(* 1999).

[12] Bravo-*Leon A* , Morikawa Y , Kawahara M , Mayo *MJ "* Fracture toughness of tetragonal zirconia with low yttria content", Acta Mater. , 50, 4555–4562(2002).

[13] C. J. Howard. , E. O. KisiOhtaka, "Crystal Structures of Two Orthorhombic Zirconias.″ J. Am. Ceram. Soc.74, 2321–23 (1991).

[14] Wyckoff R. W. G. "Crystal Structures", 2nd ed.; Wiley: New York, (1964).

[15] (a) McCullough. J. D. and Trueblood. K. N. Acta Crystallogr." The crystal structure of baddeleyite "15, 1187 **(1959**). (b) Smith DK and Newkirk HW. "The crystal structure of polymorphism of ZrO2". Acta Crystallographica 18(6) 983-991(1965) .

[16] Finnis. M. W., Paxton . A. T, Methfessel . M . Mvan Schilfgaarde "Crystal Structures of Zirconia from First Principles and Self Consistent Tight Binding". Phys. Rev. Lett. 81, 5149 (1998).

[17] Ciraci. S, Baratoff . A, Batra . I. P, "Theory of the Bimetallic Interface". Phys. Rev. B ,42, 7618 (1990).

[18] J. A. Kubby, Y. R. Wang, W. Greene." Electron interferometry at hetero junction interface". J. Phys. Rev. Lett. 65 , 2165-2168 (1990).

[19] Diebold .U."The *surface science* of titanium dioxide". Surf. Sci. Rep. 48, 53-229 (2003) .

[20] Hebenstreit .M. Li, W , Gross. L, Diebold U, Henderson. M. A, Jennison D. R, Schultz. P. A , Sears. M. P. " The *Surface Science* of Metal Oxides". Surf. Sci. 437, 173-190 (**1999**) .

[21] Ozgur. U, Alivov .YI , . Liu. C, Take. A , Reshchiko. MA. Dogan v, S , Avrutin .V, Cho .SJ ,Markoc .H. "Comprehensive Review of ZnO Materials and Devices". J. Appl. Phys. 98, 041301 (2005).

[22] Joo. J, Kwon. SG , Yu .JH , Hyeon. T. "Synthesis of ZnO Nanocrystals with Cone, Hexagonal Cone, and Rod Shapes via Non-Hydrolytic Ester Elimination Sol–Gel Reactions" .Advanced Materials 17 (15), 1873-1877(2005).

[23] F. Qu, Jr . DR. Santos, NO.Dantas, AFG. Monte, PC.Mohgttttrais, "Effects of nanocrystal shape on the physical properties of colloidal ZnO quantum dots". Physica E. 23 *(3),* 410-*415*, (2004).

[24] Kohls. M, Schmidt. T, Katschorek. H, Spanhel. L, Muller. G , Mais N, Wolf. A.Forchel. "A simple colloidal route to planar micro patterned Er @ZnO amplifiers". Adv. Mater. 11(4) 288-292 (1999).

[25] Tong, Y.H., Liu, *Y.C.*, Lu, S.X., Dong, L., Chen, S.J. *and.* Xiao, Z.Y. "The optical properties of ZnO nanoparticles capped with polyvinyl butyral". J Sol-Gel. Sci Tech, 30, 157-61(2004).

[26] Ohno .H, Munekata. H, Penney. T, Molnar.SV. Chang. LL. Magneto transport properties of p-type (In,Mn)As diluted magnetic III-V semiconductors. Phys. Rev. Lett. 68, 2664-2667 (1992).

[27] Schneider. P.M , Fowler. W.B. Physical Review Letters ." Band Structure and Optical Properties of Silicon Dioxide". Physical Review Letters, 36, (8), 38,425-428 (1976).

[28] Anderson. J.H, Parks. G.A . “The Electrical Conductivity of Silica" .The Journal of Physical Chemistry. 72:3662-8 (1998) .

[29] Chunzhao Li and Brian C. Benicewicz. "Synthesis of Well-Defined Polymer Brushes Grafted onto Silica Nanoparticles via Surface Reversible Addition−Fragmentation Chain Transfer Polymerization" Macromolecules .38,5929- 5936 (2005).

[30] Yang. H, Zhang .S, Yang .W, Chen. X, Zhuang .Z, Xu. J, Wang X."Molecularly imprinted sol-gel nanotubes membrane for biochemical separations" Journal of the American Chemical Society 126 (13), 4054-4055 (2004).

[31] Guo. H, Qian. H, Sun. S, Sun . D, Yin .H , Cai. X , Liu. Z, Wu. J, Jiang .T, Liu .X. " Hollow mesoporous silica nanoparticles for intracellular delivery of fluorescent dye "Chemistry Central Journal .5,1 (2011).

[32] S. V. Han, D. H. Lee, V. J. Chang, S. O. Ryu, T. J. Lee, C. H. Chang., "The Growth Mechanism of Nickel Oxide Thin Films by Room-Temperature Chemical Bath Deposition" .Journal of the Electrochemical Society 153(6), C382-C386 (2006).

[33] Li .Q. Y, Wang. R. N, Nie .Z. R, Wang .Z. H, Wei. Q." Preparation and characterization of nanostructured $Ni(OH)_2$ and NiO thin films by a simple solution growth process". Journal of Colloid and Interface Science 320 , 254-258 (2008).

[34] Krishnakumar. S. R, Liberati. M, Grazioli. C. Veronese .M , Turchini. S, Luches. P, Valeri. S, Carbone .C.," Magnetic linear dichroism studies of in situ grown NiO thin films" J. of Magnetism and Magnetic Materials 310, 8-12 (2007) .

[35] Kuen-Ming Shu, Tu .G.C.. "The microstructure and the thermal expansion characteristics of Cu/SiC composites" Materials Science and Engineering . A349, 236-247 (2003) .

[36] J. Lu, Z.Ye , L. Wang ,J.Huang, B.Zhao. " Structural, electrical and optical properties of N-doped ZnO films synthesized by SS-CVD". Materials Science in Semiconductor Processing, 5, 491 - 496(2003).

[37] B.Pejova, T. Kocareva, M. Najdoski, I.Grozdanov." A solution growth route to nanocrystalline nickel oxide thin film". Applied Surface Science .165 (4), 271-278 (2000).

[38] Lopez .T, Mendez. J, Mudio .T. Z. and Villa. M. "Spectroscopic study of sol-gel silica dopped with iron ions " . Materials Chemistry and Physics (Elsevier). 30 , 161 (1992).

[39] Hammond .C." The Basic of Crystallography and Diffraction" ; Oxford University Press; New York, NY, (1997).

[40] Zha .M, Calestani. D, Zappettini.A . "Large-area self-catalysed and selective growth of ZnO nanowires" Nanotechnology 19 (32), 325603 (2008).

[41] Balog. M., Schieber .M., M. Michman, Patai .S.. "The chemical vapour deposition and characterization of ZrO2 filmsanometalic compounds" from org Thin Solid Films .47, 109 -120 (1977).

[42] Ashwani Sharma, Pallavi, Sanjay Kumar, "Synthesis and Characterization of NiO-ZnONanocomposites "Nano Vision 1(3) 115-122. (**2011**) .

[43] Mahmoudi .H. Chenari, M. Ali Hassanzadeh,. Golzan. M., . Sedghi.,H. Talebian M.." Frequency dependence of ultrahigh dielectric constant of novel synthesized SnO_2 nanoparticles thick films" .Current Applied Physics. 11, 409-413 (**2011**).

[44] C. Prakash and J S. Bajal . J. Less Common Metals . "Dielectric behaviour of tetravalent titanium-substituted Ni-Zn ferrites" .Journal of the Less Common Metals 107 (1), 51-57 (**1985**).

[45] D. Ravinder . "Effect of sintering temperature on the dielectric behaviour of lithium ferrite "Phys Status Solidi (a)139(1):K69 - K72 (1993).

[46] Ramana Reddy .A V., Ranga Mohan .G., Ravinder. D. and Boyanov .B. S. , "High-Frequency Dielectric Behaviour of Polycrystalline Zinc Substituted Cobalt Ferrites," .J. Mater. Sci. 34 ,3169 - 3176 (1999).

[47] Kumar, G. B. and Buddhudu, S." Optical, thermal and dielectric properties of Bi 4 (TiO 4) 3 ceramic powders". Ceram. Int. 36,1857-1861 (2010).

Table 1: Composition of Different Mixes in mol%

Oxides	ZnO mol%	NiO mole%	SiO_2 mole%	ZrO_2 mole%
Z_1	39	30	30	1
Z_2	38	30	30	2
Z_3	37	30	30	3
Z_4	36	30	30	4
Z_5	35	30	30	5
Z_6	30	30	30	10

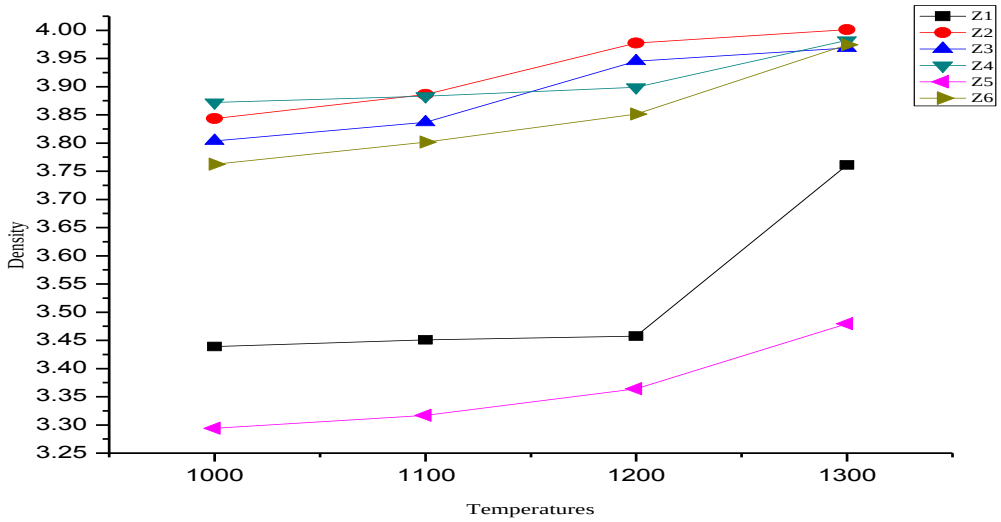

Fig .1. Relative density as a function of temperature

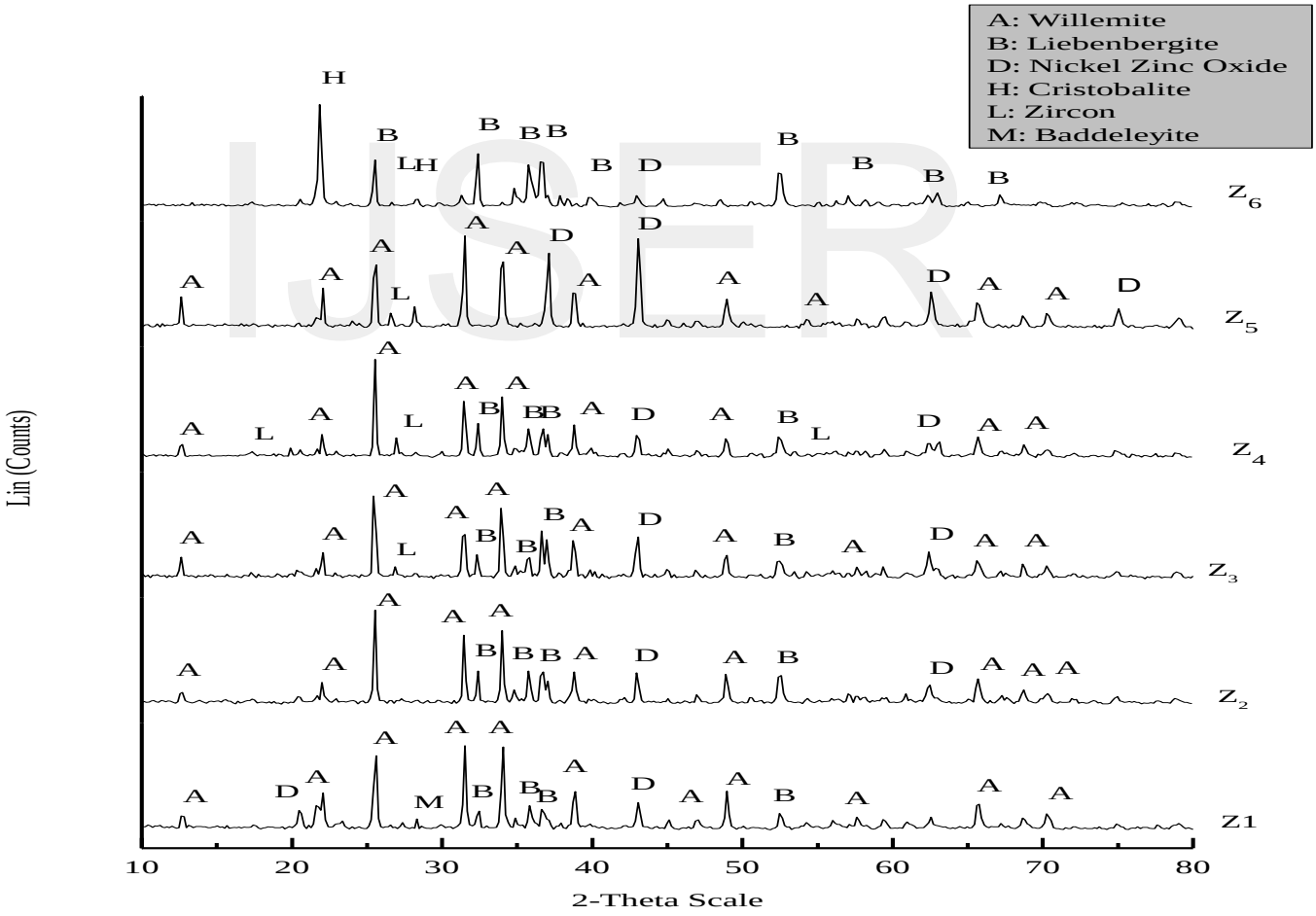

Fig.2. XRD of group (III) sintered at 1200°C

Where A : willemite $Zn_2(SiO_4)$,M: Baddeleyite ZrO2 ,L : Zircon Zr(SiO4), B: Liebenbergite Ni_2SiO_4, D: Nickel zinc oxide

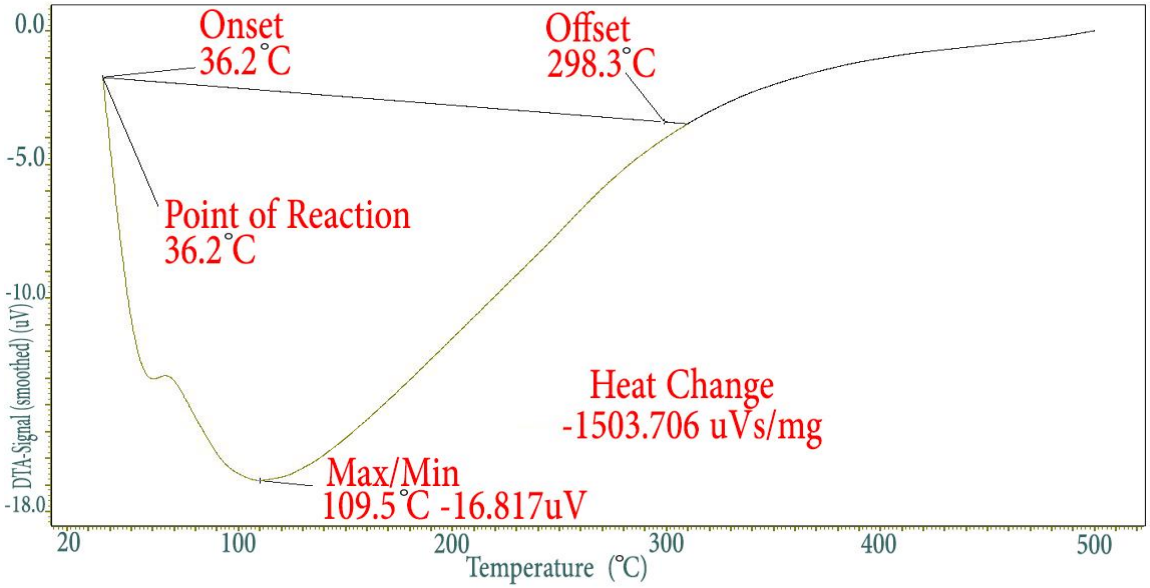

Fig. 3. shows the DTA thermogram of sample Z_6

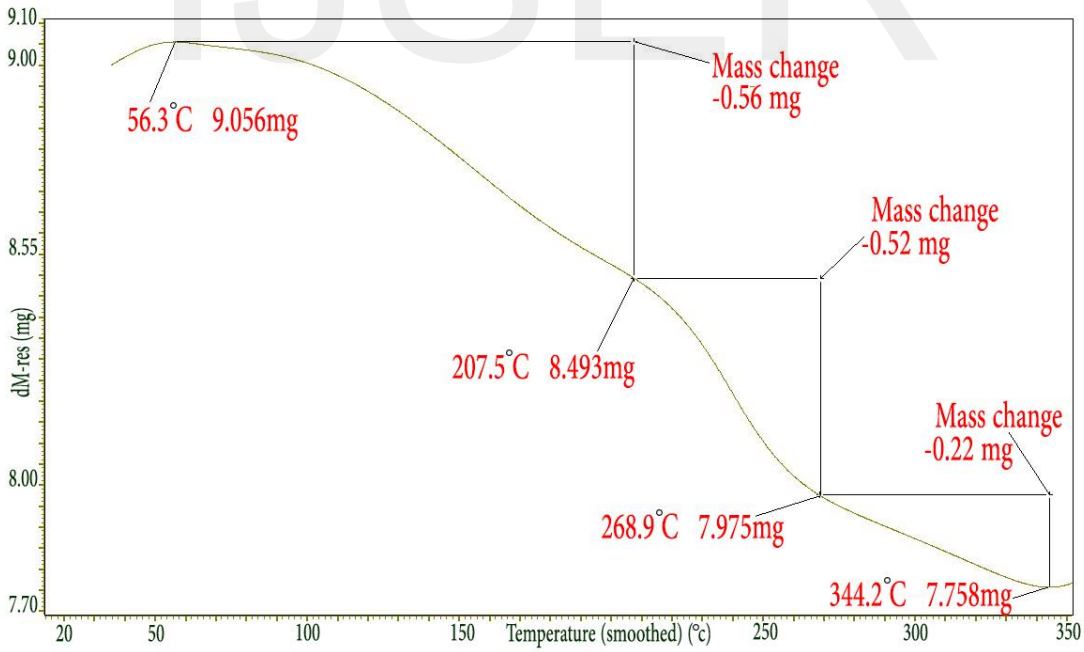

Fig.4 . shows the TG thermogram of sample Z6

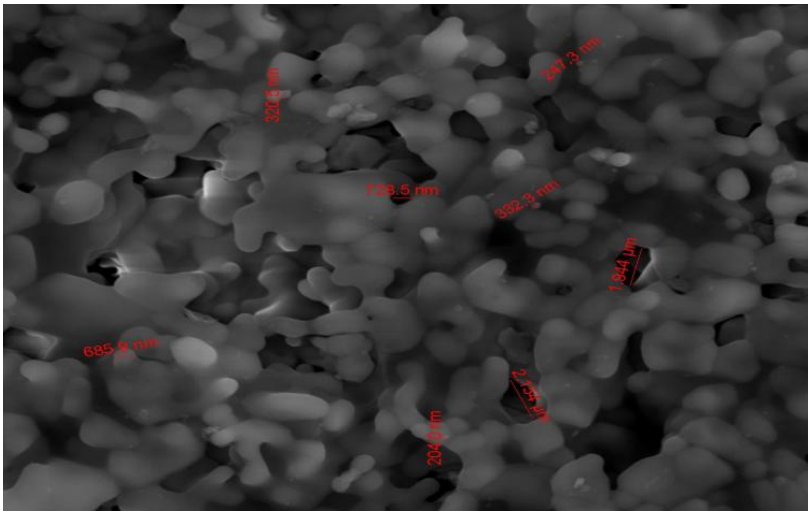

Fig.5 . SEM of sample Z1 at 1100 ^{0}C , thermally etched surface, showing crystal growth of ZnO grains and the presence of liquid phase X=10000

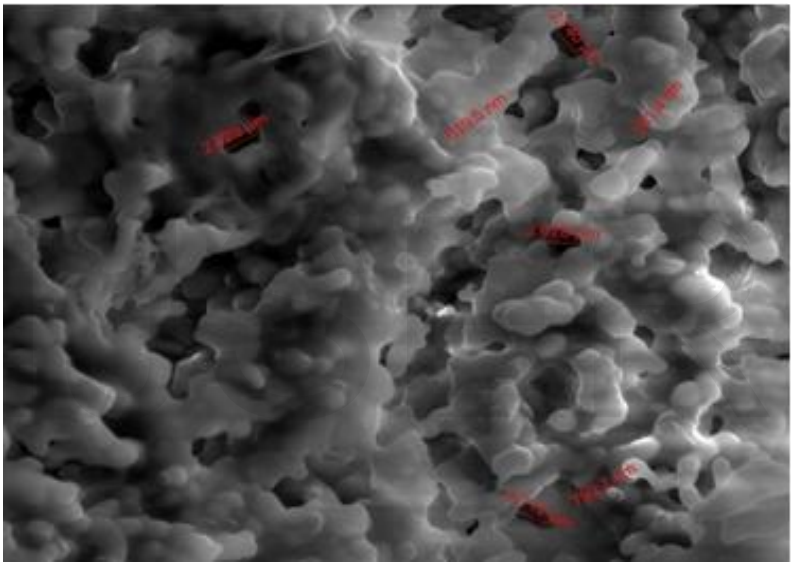

Fig.6.SEM of sample Z1 at 1200^{O}C for 2h , X= 5000

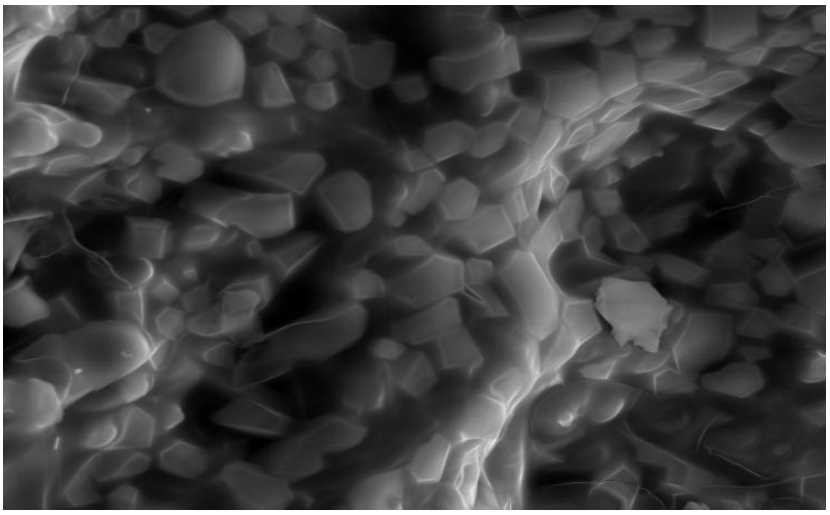

Fig . 7. SEM of sample Z1 at 1300^{O}C for 2h X=3000(crystalline phase)

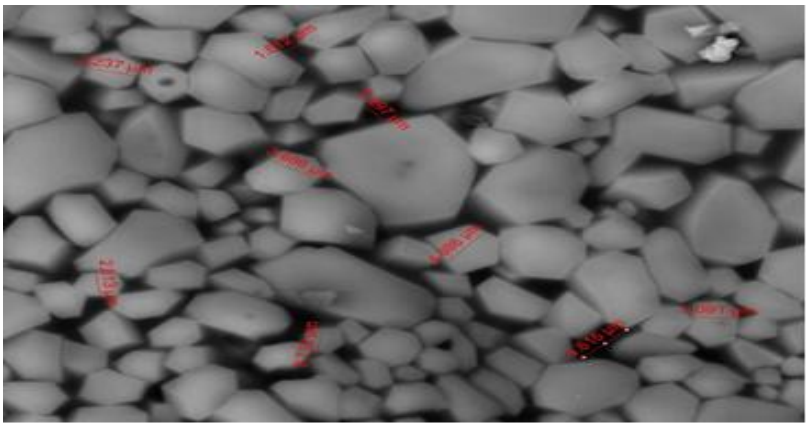

Fig.8 .SEM of sample Z1 at 1300^{O}C for 2h X=5000 (crystalline phase)

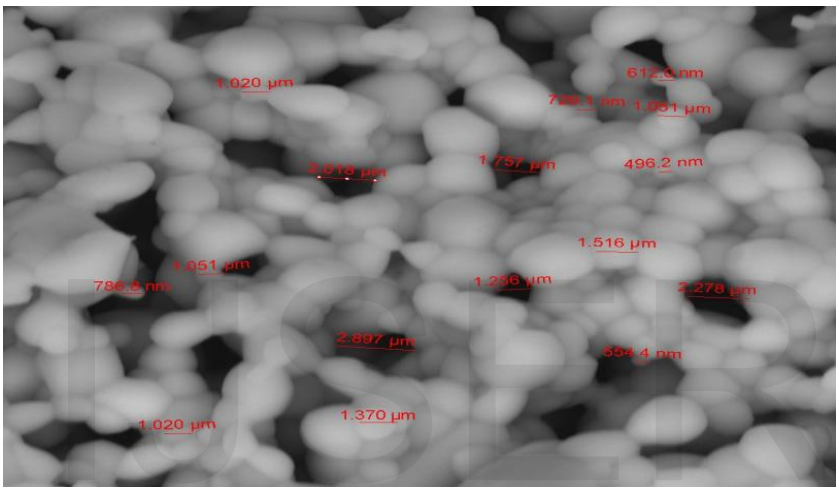

Fig.9 .SEM of sample Z4 at 1000^{O}C for 2h X=10000

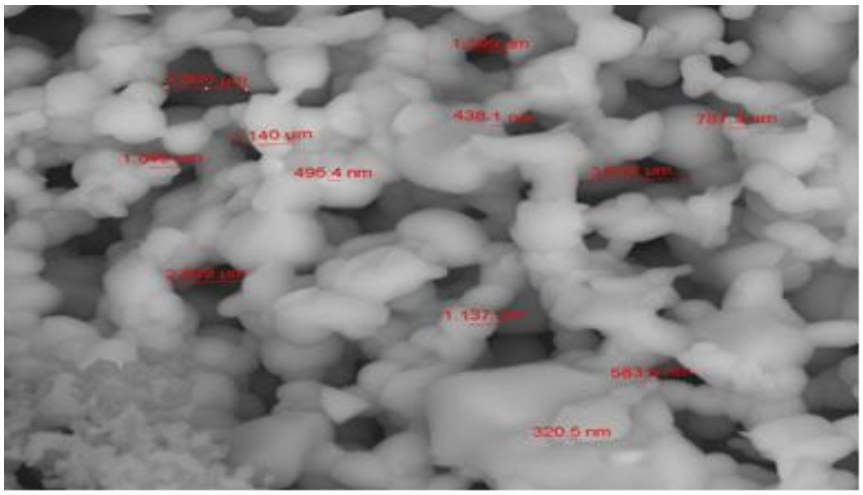

Fig.10.SEM of sample Z4 at 1100^{O}C for 2h , X=10000

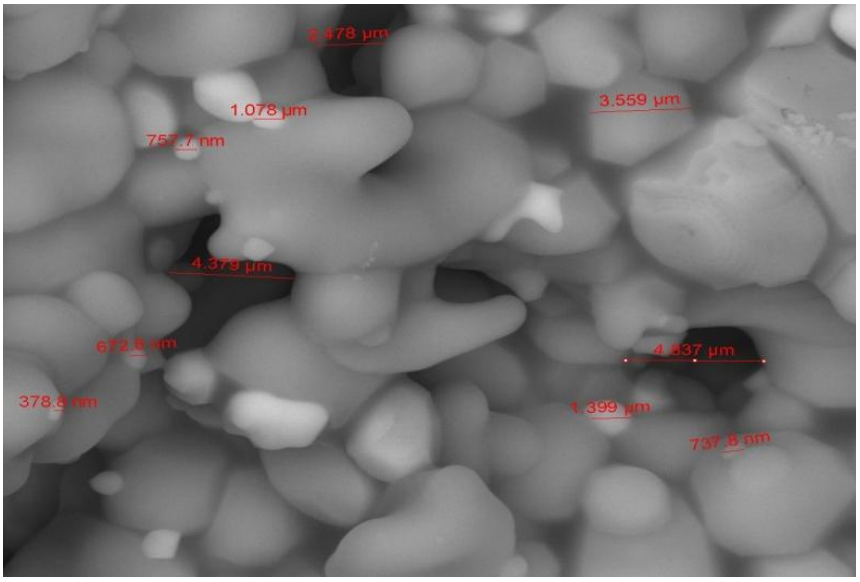

Fig.11. SEM of sample Z4 at 1200^{O}C for 2h X=10000

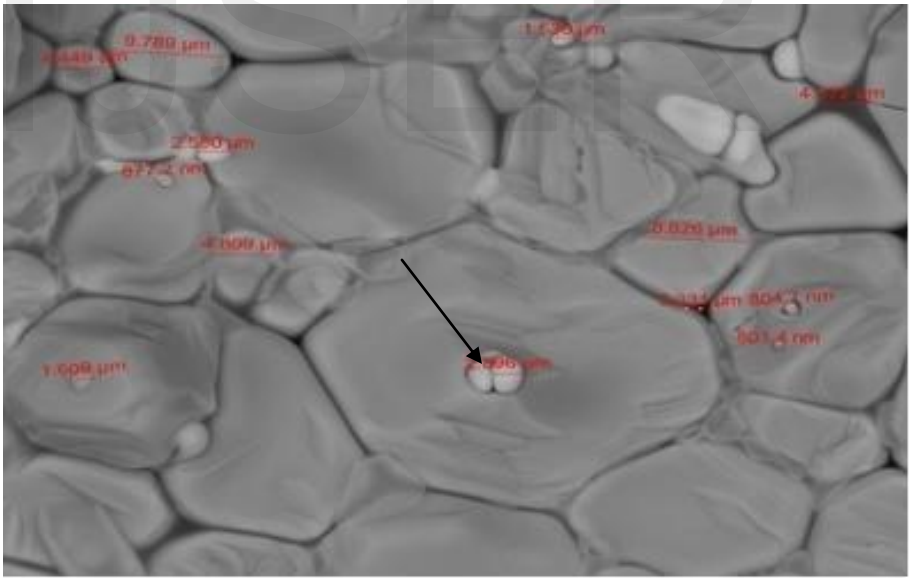

Fig.12.SEM of sample Z5 at 1300^{O}C for 2h (growth grains), the grain boundaries as well as the domain structure are visible after thermal etching , X=5000

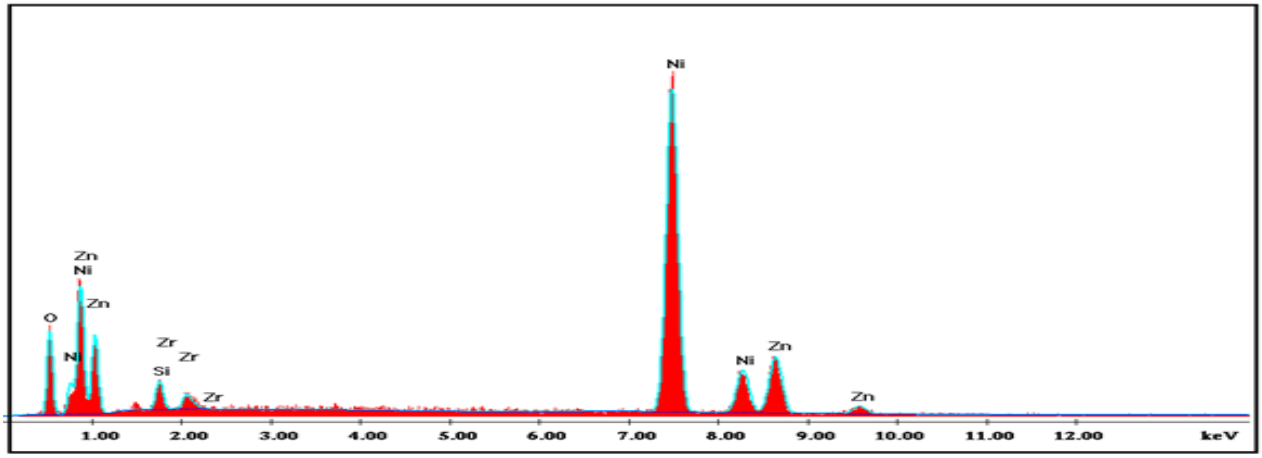

Fig .13. EDAX of sample Z5 at 1300 shows distribution of elements.

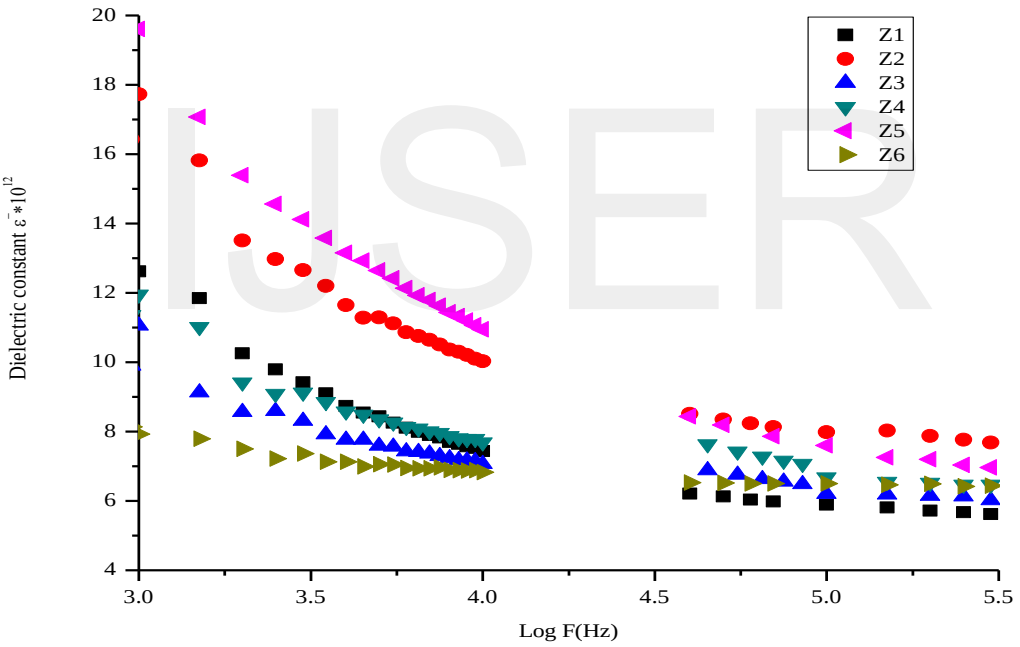

Fig. 14 . AC Dielectric constant as a function of frequency for different mixes sintered at 1200°C.

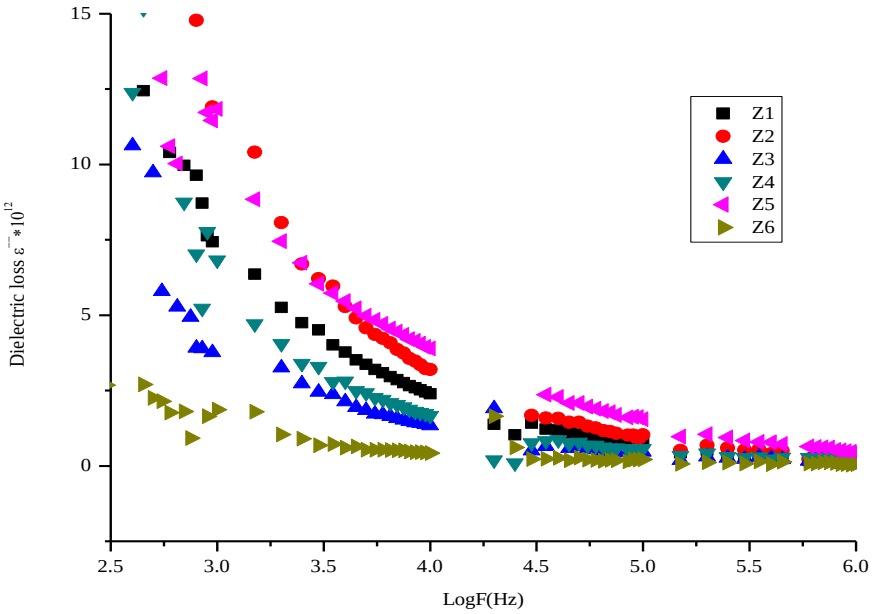

Fig. 15 . AC Dielectric loss as a function of frequency for different mixes sintered at 1200°C

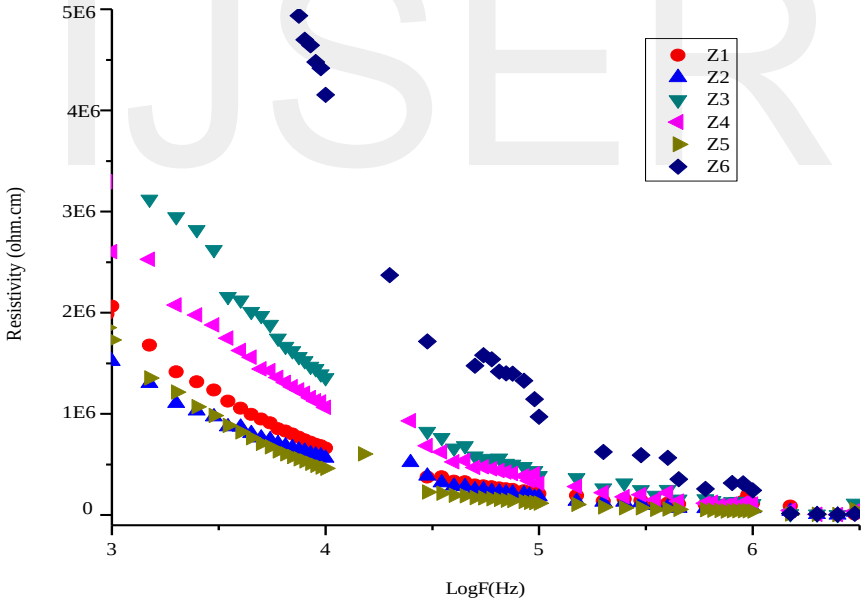

Fig.16 . Resistivity as a function of frequency for different mixes sintered at 1200°C